

Hydrothermal analysis of water- Al_2O_3 nanofluid flow through a sudden expansion channel with an intermediate step

Sandip Saha^{1,*}, Apurba Narayan Das²

¹ *Division of Mathematics, School of Advanced Sciences, Vellore Institute of Technology Chennai, Chennai-600127, Tamilnadu, India*

² *Dept. of Mathematics, Alipurduar University, Alipurduar-736121, West Bengal, India*

* *Corresponding author: sandip.tfgss@gmail.com*

Abstract

This work presents the dynamic behavior of the laminar hydrothermal flow of nanofluid through a sudden expansion channel with the variations in the normalized length, height, and pitch to width ratio of the intermediate step. The governing equations have been discretized using the finite volume method, and the SIMPLE algorithm has been applied to solve the system of algebraic equations. The effect of the variations in the Reynolds number (Re), normalized height (B/C), normalized length (A/C), and step pitch-width ratio (A/B) on the enhancement of heat transfer has been studied. For different values of A/C , A/B , and B/C , this work indicates that the average Nusselt number (Nu_{avg}), thermal resistance factor (R), and performance number (PN) increase with the increase in Re . In the case of the hydrothermal flow phenomena, the configuration associated with B/C provides better results than those associated with A/B and A/C . As an important outcome, we see that the presence of an intermediate step enhances the average Nusselt number and thermal resistance factor. This will become very much helpful for various realistic circumstances for triggering additional thermo-mechanical loads on the surface.

Keywords: Friction factor; intermediate step; laminar flow; performance number; thermal resistance factor.

1. Introduction

Transport of nanofluid flow and heat transfer phenomena through sudden expansion channels and rectangular channels have wide applications in different engineering appliances [Al-Ashhab (2019); Al-Hajri *et al.* (2020); Saha *et al.* (2020); Wei *et al.* (2020); AL-Jawary (2020); Saha *et al.* (2021a); Kiran *et al.* (2021); Saha *et al.* (2021b)]. Several authors have studied different characteristics of HT phenomena through various types of the channel in the presence of porous media [Joibary & Siavashi (2019); Norouzi *et al.* (2020); Rashidi *et al.* (2019)]. Generally, porous media is used in the channels to increase the rate of HT. Flow through a sudden expansion channel is a well-known phenomenon [Mostafavi & Meghdadi (2017)]. Many authors [Menouer *et al.* (2019)], experimentally and numerically, have shown that the increase in Re causes the existence of two or more flow separation zones at the lower and upper corner walls,

which causes a substantial heat loss [Galuppo & De (2017)]. Hilo *et al.* (2020) studied different properties of the hydrothermal phenomena of flow over a suddenly expanded channel. To enhance the rate of HT, many researchers [Rashidi *et al.* (2019); Boudiaf *et al.* (2020)] have investigated the hydrothermal phenomena using nanofluid and stated that the rate of HT can be enhanced using nanofluid instead of the base fluid. In a sudden expansion channel with porous suction, Terekhov & Terekhov (2017) discussed the flow separation region and stated that an increase in the strength of transverse mass flux shortens the separation region in suction and lengthens the same in blowing. Dyachenko *et al.* (2019) investigated the profiles of Δp in the separation zone forms after the expanded section of a suddenly expanded channel with vortex generators. They stated that the rate of HT increases with the enhancement of vortex lengths. Naphon (2007) experimentally investigated the different characteristics of heat transfer through a V-shaped sudden expansion channel. It is demonstrated that after the recirculation zone the mixing of the fluid in the boundary layer intensifies, which increases convective HT. In addition, he studied that the breaking of the thermal boundary layer could increase the rate of HT when the flow past the corrugated surfaces. Through various types of corrugated channels, Ajeel *et al.* (2019) studied the thermal enhancement of nanofluid flow phenomena. They concluded that the pressure drop and recirculation characteristics depend on the shape of the teeth. It has also been shown that the value of Nu_{avg} increases with the increase in Re . In an abruptly changed channel, Maghsoudi & Siavashi (2019) showed that the value of Nu_{avg} found in the case of a smooth channel increases by 8.3% for the presence of porous insert. In the presence of a porous floor segments in a sudden expansion channel, Abu-Hijleh, (2000) investigated the reattaching flow characteristics. They concluded that the value of Nu_{avg} found in the case of a smooth channel increases by 16% for the existence of porous media. Martin *et al.* (1998) numerically analyzed the hydrothermal phenomena through a sudden expansion channel with a porous medium. They concluded that thermal behavior enhances with the increase in the height of the porous medium.

In this work, we have studied the effect of the variations in A/B , B/C , and A/B on flow phenomena, and this will be helpful to form thermo-mechanical machines at low production costs. Nanofluid has better heat transfer enhancement compared to any base/Newtonian fluid for having a higher thermal conductivity of the nanoparticles and is used in many engineering equipment. From the above literature survey, it has been found that no work has been done on nanofluid flow and the rate of HT phenomena through sudden expansion channel with intermediate step. This provides us enough confidence to carry forward the current work. The present work is an extension of the studies of Ternik *et al.* (2006). They studied the flow phenomena of power-law fluids without considering HT phenomena and the effect of the intermediate step. In this work, we have investigated the water-Al₂O₃ nanofluid flow phenomena and HT characteristics including streamlines, F , Nu_{avg} , R , and PN with the variations of A/B , B/C , A/B , and Re in a two-dimensional sudden expansion channel with intermediate step.

2. Geometry of the problem

The flow geometry of the physical domains has been presented in the figures. 1(a-b), where the flow enters through the inlet with velocity, u_{in} at the temperature, T_{in} . Figure. 1(a) presents the flow geometry of the suddenly expanded channel and figure 1(b) presents the computational domain with an intermediate step. The flow is assumed viscous, incompressible, steady, single phase, laminar, and the particles have no inertia and the radiation of HT has been neglected. Constant heat flux has been assigned to the lower wall only, and other walls have been kept insulated.

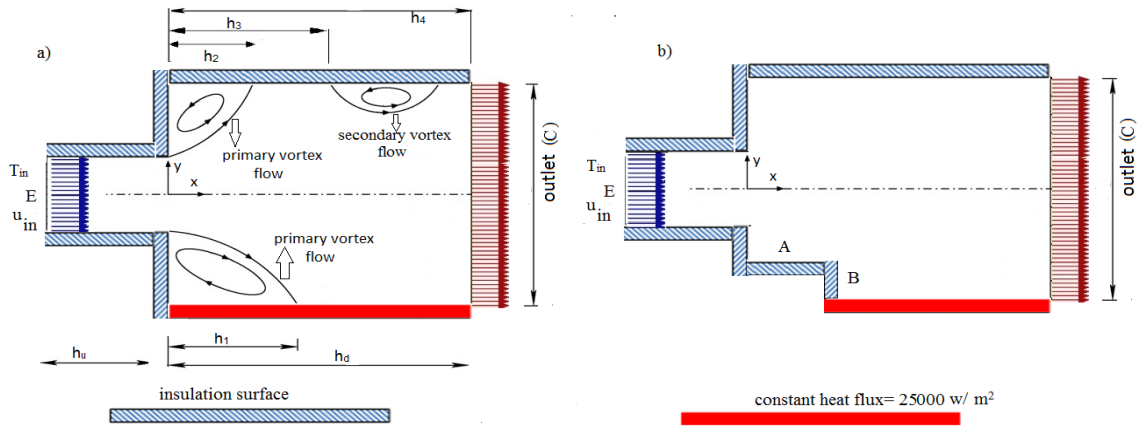


Fig. 1. Geometry without (a) intermediate step and with (b) intermediate step.

3. Formulation of the Problem

The following non-dimensional equations have been used to analyze the hydrothermal phenomena of fluid flow in the Cartesian coordinate system [Aminossadati *et al.* (2011); Akbari *et al.* (2015); Behnampour *et al.* (2017)].

$$\text{Continuity equation:} \quad \frac{\partial U}{\partial X} + \frac{\partial V}{\partial Y} = 0 \quad (1)$$

$$\text{The momentum of X equation:} \quad U \frac{\partial U}{\partial X} + V \frac{\partial U}{\partial Y} = \frac{\mu_{nf}}{\rho_{nf} \nu_f} \frac{1}{Re} \left(\frac{\partial^2 U}{\partial X^2} + \frac{\partial^2 U}{\partial Y^2} \right) - \frac{\partial P}{\partial X} \quad (2)$$

$$\text{The momentum of Y equation:} \quad U \frac{\partial V}{\partial X} + V \frac{\partial V}{\partial Y} = \frac{\mu_{nf}}{\rho_{nf} \nu_f} \frac{1}{Re} \left(\frac{\partial^2 V}{\partial X^2} + \frac{\partial^2 V}{\partial Y^2} \right) - \frac{\partial P}{\partial Y} \quad (3)$$

$$\text{Energy equation:} \quad U \frac{\partial \theta}{\partial X} + V \frac{\partial \theta}{\partial Y} = \frac{\gamma_{nf}}{\gamma_f} \frac{1}{Re} \frac{1}{Pr} \left(\frac{\partial^2 \theta}{\partial X^2} + \frac{\partial^2 \theta}{\partial Y^2} \right). \quad (4)$$

Where the following non-dimensional parameters have been used:

$$X = \frac{x}{E}, Y = \frac{y}{E}, \theta = \frac{T - T_{in}}{\Delta T}, \Delta T = \frac{25000 E}{k_f}, Re = \frac{\rho_f u_{in} E}{\mu_f}, U = \frac{u}{u_{in}}, V = \frac{v}{u_{in}}, Pr = \frac{\theta_f}{\gamma_f}, P = \frac{p}{\rho_{nf} u_{in}^2}.$$

3.1 Boundary conditions

At the inlet section: $X = -2$, $-1.5 < Y < 1.5$, $U = 1$, $\theta = 0$, and at the outlet section: Outflow boundary conditions; $\frac{\partial U}{\partial X} = 0$, $\frac{\partial V}{\partial X} = 0$ and $\frac{\partial \theta}{\partial X} = 0$ have been imposed and finally, at the wall section: No slip ($U_X = 0$, $V_X = 0$) and no penetration ($U_Y = 0$, $V_Y = 0$) boundary conditions have been implemented at the walls and a constant heat flux has been applied at the lower wall but the other walls remain insulated ($\frac{\partial \theta}{\partial X} = 0$).

4. Characteristics of Nano fluid

The following equations have been used to calculate the ρ_{nf} and $(\rho C_p)_{nf}$ [Behnampour *et al.* (2017)].

$$\rho_{nf} = (1 - D)\rho_f + D\rho_s \quad (5)$$

$$(\rho C_p)_{nf} = (1 - D)(\rho C_p)_f + D(\rho C_p)_s \quad (6)$$

The following mean empirical correlation [Patel *et al.* (2005); Behnampour *et al.* (2017)] is used to evaluate the k_{ef} .

$$k_{ef} = k_f + k_f \frac{k_s D}{k_f (1 - D)} [1 + 36000 Pe] \quad (7)$$

Thermo-physical properties of nanofluid have been taken from the studies of Corcione (2010) and Akbari *et al.* (2016).

5. Computational procedures, the test of grid and validation of the model

The computational fluid dynamics solver, Fluent [Soueid *et al.* (2020)] has been utilized for simulation and visualization purposes. FVM has been utilized to solve the governing equations (equation 1-equation 3) with the aid of a second-order upwind scheme. In addition, the SIMPLE algorithm [Corcione (2010); Akbari *et al.* (2015); Behnampour *et al.* (2017)] has been used to discretize the pressure-velocity coupling. The convergence criteria have been set as 10^{-6} , 10^{-6} , and 10^{-9} for continuity, momentum, and energy equations respectively.

The whole computation domain has been segregated into two parts (figure. 2). To study the effect of mesh size, three different mesh studies and grid tests have been performed at $Re = 30$, as illustrated in figure. 3. Figure. 3(a) presents the variation in the pressure coefficient along the x-axis with the variations in the length of the channel. It is clearly shown in figure. 3(a) that the mesh 2 can be taken for future analysis and from figure. 3(b), it is investigated that 91,260 cells are sufficient for further analysis. The code validation has been done with the studies of

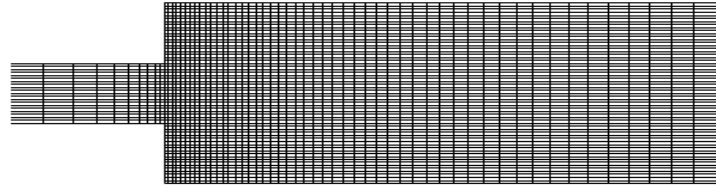


Fig. 2. Geometry of mesh.

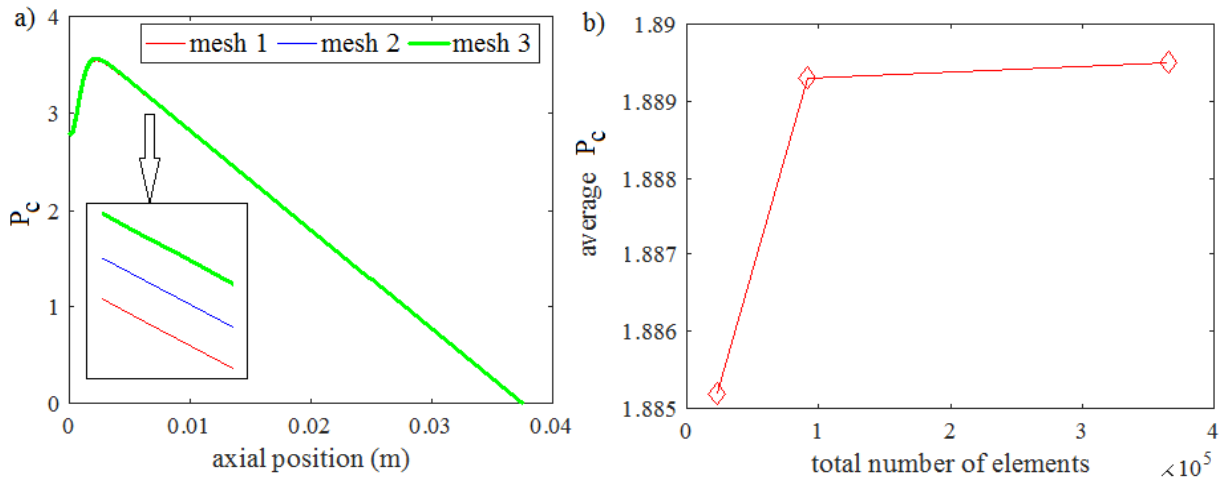


Fig. 3. Plots of (a) P_c vs. axial position and (b) average P_c vs. the total number of elements.

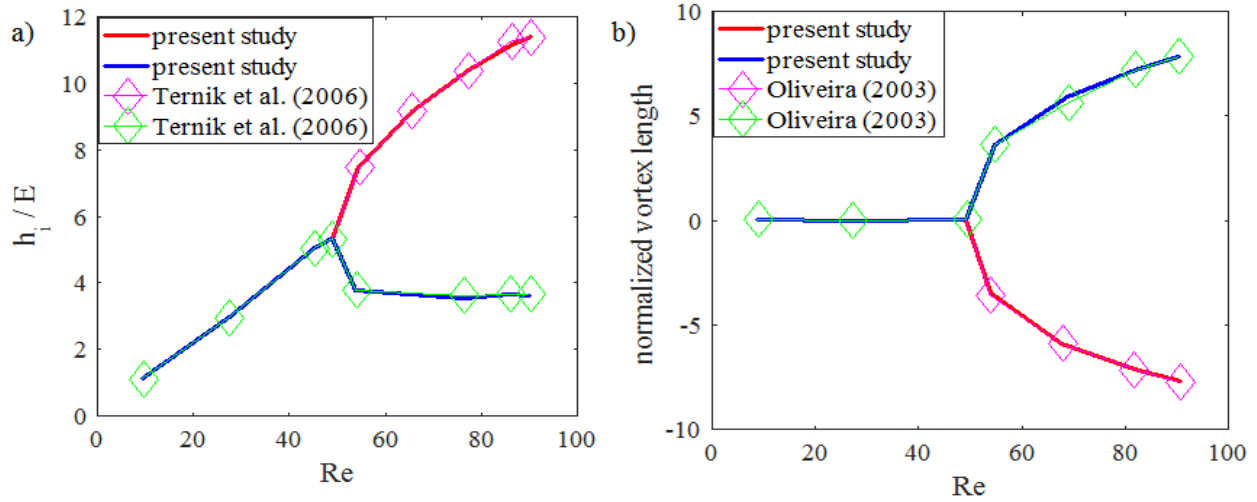


Fig. 4. Plots of (a) primary vortex length and (b) normalized vortex length vs. Re .

Oliveira (2003) and Ternik *et al.* (2006) by comparing the results of primary and normalized vortex lengths, and shows a good agreement with the present model, as can be seen in the figures. 4(a-b).

6. Results and discussions

This section describes the effect of various parameters, viz., Re , Nu_{avg} , PN , and different geometrical parameters of intermediate steps (A/B , B/C , and A/B) on the hydrothermal phenomena of flow.

6.1 Effect of B/C , A/C , and A/B on flow phenomena at $D=0\%$

The flow is separated from the lower corner of the suddenly expanded channel and creates a primary weak zone in the clockwise direction. At $Re=100$, the profiles of velocity streamlines

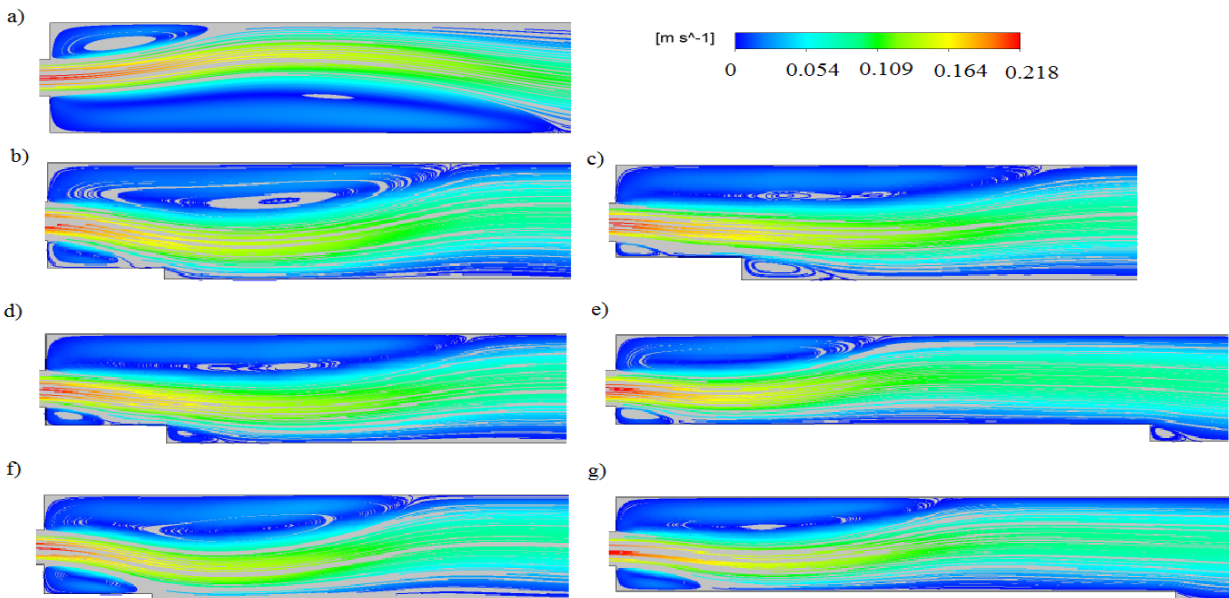


Fig. 5. Velocity streamlines for different configurations at $Re = 100$ and $D = 0\%$.

have been shown in the absence of intermediate step, i.e., for $A/B = 0$, $B/C = 0$ and $A/C = 0$ (figure. 5a), and in the presence of intermediate steps, i.e., for $A/C=0.05$ (figure. 5b), $A/C=0.2$ (figure. 5c), $B/C=1$ (figure. 5d), $B/C = 5$ (figure. 5e), $A/B = 5$ (figure. 5f) and $A/B = 30$ (figure. 5g). It is observed that the presence of intermediate step at higher values of B/C , and A/C allow the fluid to flow smoothly, which causes the existence of weak zones after the intermediate step. In addition, the size of recirculation zones is found to depend on the configurations of intermediate step. Moreover, just after the step, a weak zone of small length appears and becomes stronger as the fluid passes the steps. Furthermore, the rate of heat transfer enhances due to the existence of a second weak zone, as a result, isotherms become denser. It has been investigated that with the increase in the value of B/C , the first weak zone disappears and the length of the second weak zone increases. It has also been observed that the second weak zone disappears as the value of A/B increases. In addition, the length of the flow reattachment point increases with the increase in Re .

6.2 Effect of Re and PN

Due to the adverse pressure gradient in the sudden expansion zone, it has been noted from figure. 5(a) that the weak zone appears at both the lower and upper walls. From the figure. 5, it has been observed that velocity streamlines become slightly sparse just after the sudden expansion and also found that as it proceeds towards the outlet section, it becomes scattered indicating that due to low velocity, heat transfer rate decreases. The permeability of the streamlines near the walls reduces and heat transmission increases. As a result, the thickness of the thermal and hydrodynamic boundary layer increases. As the step height increases, the length of the weak zone also increases, as a result, the rate of heat transfer enhances slightly. Moreover, as the value of A/C increases to some specific value, the length of the weak zone continuously reduces and the same lies completely within the step. This mechanism destabilizes the heat transfer by itself, but the heat transfer is usually improved by having higher thermal conductivity. The effects of Re , A/B , A/C , and A/B on Nu_{avg} , F have been shown in the figures. 6(a-e). In all the considered cases, it has been found that the increase in Re , B/C , A/C , and A/B causes an increase in Nu_{avg} [figures. 6(a-c)] and decrease in F (figures. 6(d-e)). The profile of F depends on the values of Δp . Due to the effect of viscous dissipation, Δp increases monotonically and causes enhancement of heat transfer. The value of Nu_{avg} attains its maximum at the zone surrounding the attachment point, and these points move the downstream with the increase in Re . Generally, the increased values of Re are correlated with the increased shear stress. At $Re = 300$ and $D = 0\%$, it has been revealed that the value of Nu_{avg} enhances by 56% at $B/C = 0.33$ of that at $B/C = 0$. At $Re = 300$ and $D = 4\%$, it has also been studied that the value of Nu_{avg} reaches approximately 1.46 times at $A/C = 15$ of that at $A/C = 1$, and at $A/B = 50$, the value of Nu_{avg} increases up to 1.438 times of that at $A/B = 10$, as can be seen from the figures. 6(a-c). It has also been investigated that the plots of Nu_{avg} , and F become more pronounced with the increase in $D\%$. At $Re = 300$, the figure. 7 shows the variation in R with D for different configurations of the intermediate step. The profile of R has been described as an efficient parameter of thermal enhancement. It is noted that the value of R increases with the increase in the values of B/C (figure. 7a), A/C (figure. 7b), and $D\%$. The value of thermal enhancement factor starts to increase due to the enhancement in the cooling effect by reducing the wall temperature at the downstream section. Consequently, the boundary-layer thickness decreases. At $Re = 300$, $B/C = 0.33$ and $D = 4\%$, it has been found that the value of R increases up to 1.2 times of that at $D = 0\%$, while at $A/C = 7$, it becomes 1.12 times of that at $D = 0\%$. Effects of different geometric parameters of intermediate steps on the performance number have been shown in the figures. 8(a-c). For the values of B/C , the boundary layer of the lower wall occupies a significant portion of the step, particularly at a low velocity. As the value of B/C increases, a large portion of the fluid tends to flow through the intermediate step. The use of a porous medium can prevent the sudden increase in Nu_{avg} at the reattachment point, which is unacceptable in many realistic contexts for triggering additional thermo-mechanical loads on the material surface. Moreover, the thickness of the step, rather than the porosity or permeability of the porous material, has a greater effect on the flow and heat transfer

characteristics. In all the considered cases, it has been noted that the performance number reaches greater than one, implying a greater thermal enhancement.

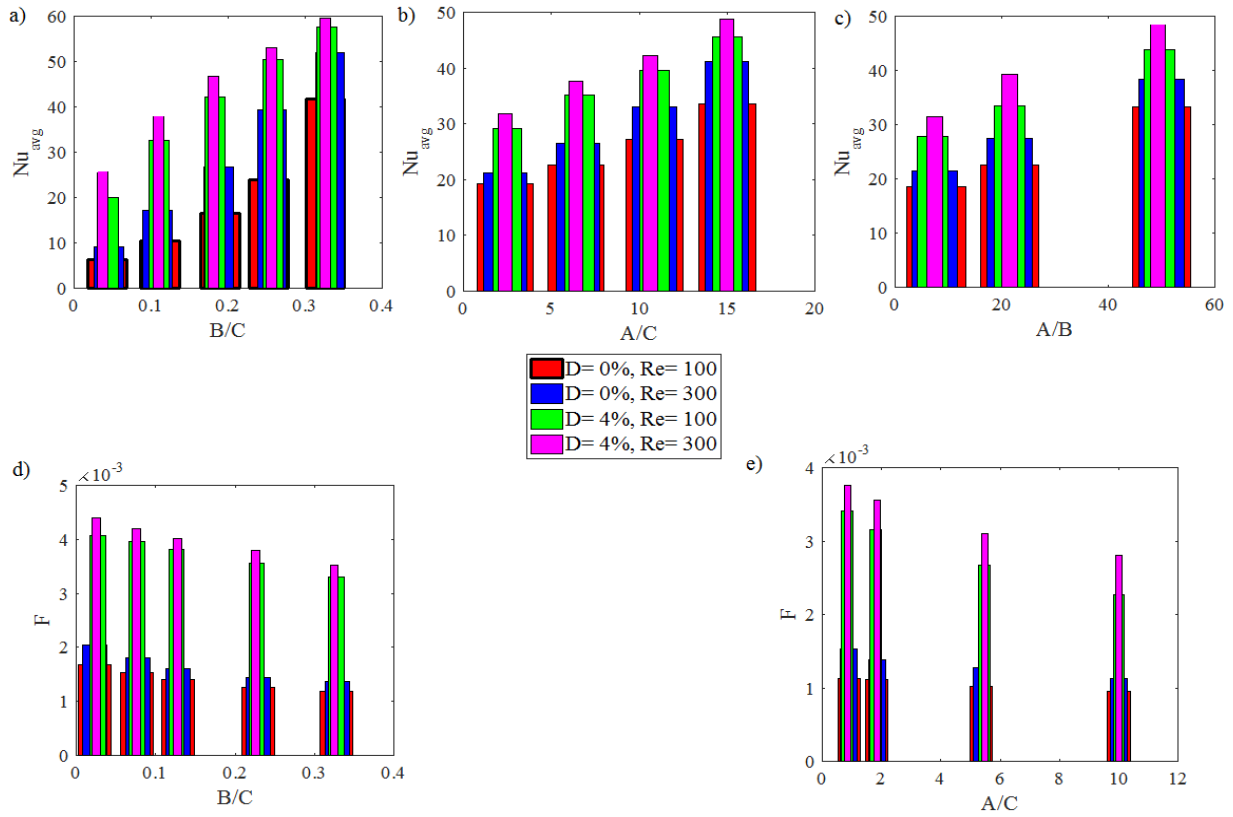


Fig. 6. Variations of (a-c) Nu_{avg} and (d-e) F at $Re = 100, 300$ for $D=0\%$ and 4% .

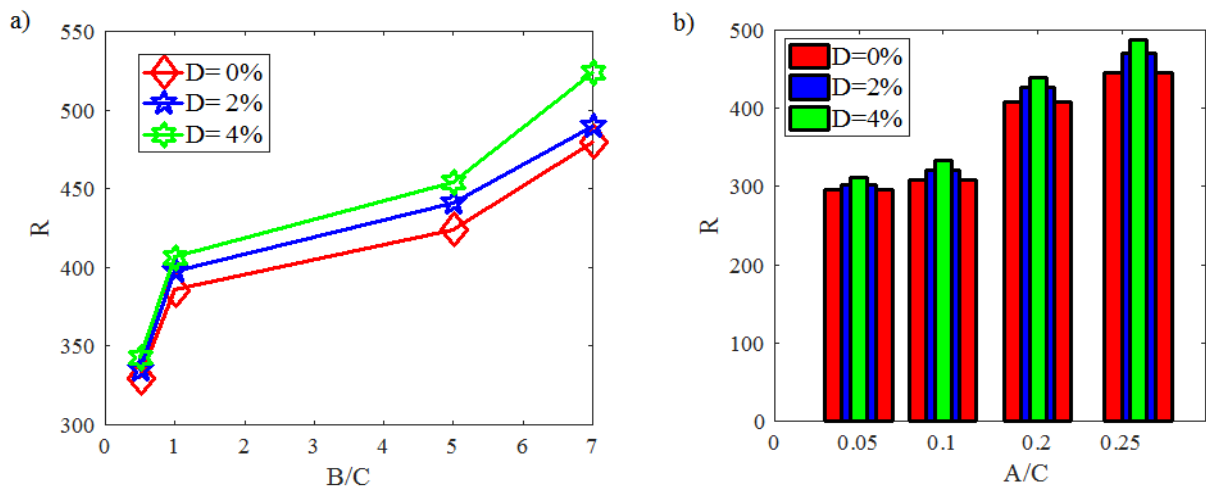


Fig. 7. Variations of R for different configurations at various D .

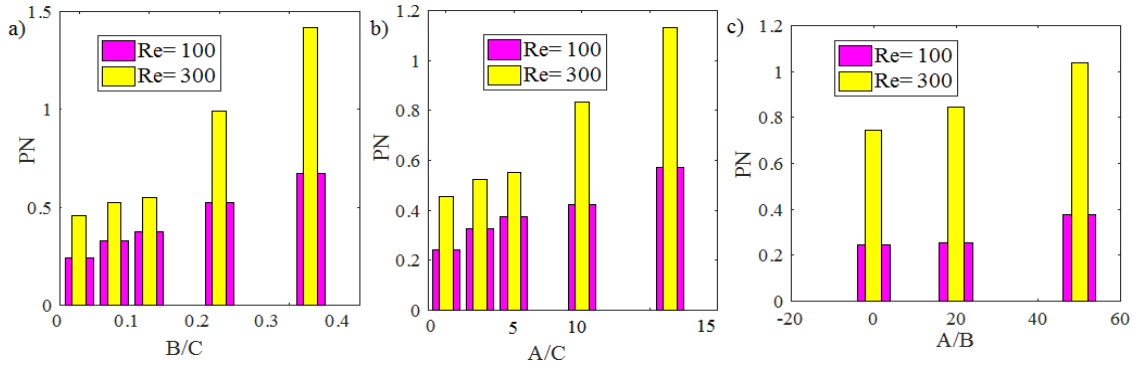


Fig. 8. Bar diagrams of PN for different configurations at $Re = 100$ and 300 and $D = 4\%$.

7. Conclusions

A numerical study has been performed to investigate the influence of intermediate step with limited length, height, and pitch-width ratio on the enhancement of heat transfer phenomena. The major findings of the present work are as follows:

(a) Enhancement of heat transfer causes the enhancement in Re , percentage of volume fraction of nanoparticles, normalized step height, normalized step length, and pitch-width ratio. An increase in Re causes an increase in the average Nusselt number and performance number. In the case of thermal enhancement, the following configurations have been followed:

B/C (normalized height of intermediate step) $>$ A/C (step pitch to width ratio) $>$ A/B (normalized length of intermediate step).

(b) A porous medium can prevent the sudden increase in Nu_{avg} at the reattachment point, which is unacceptable in many realistic contexts for triggering additional thermo-mechanical loads on the material surface.

(c) To enhance the heat transfer, the use of a porous block or the use of bell surface in a thermo-mechanical model is too expensive, but the present study suggests that the presence of the intermediate step in a sudden expansion channel reduces the cost, which becomes very much helpful for the engineering communities related to flow phenomena.

References

Abu-Hijleh, B. A. (2000) Heat transfer from a 2D backward facing step with isotropic porous floor segments. *Int J Heat Mass Transf*, 43: 2727-2737.

Ajeel, R. K., Salim, W. S. & Hasnan, K. (2019) Thermal performance comparison of various corrugated channels using nanofluid: numerical study. *Alex Eng J*, 58: 865-877.

Akbari, A. O., Toghraie, D., Karimipour, A., Safaei, R. M., Goodarzi, M., Alipour, H. & Dahari, M. (2016) Investigation of rib's height effect on heat transfer and flow parameters of laminar water - Al₂O₃ nanofluid in a rib-microchannel. *Applied Mathematics and Computations*, 290: 135-153.

Akbari, O. A., Karimipour, A., Toghraie, D. Karimipour, A. (2015) Impact of ribs on flow parameters and laminar heat transfer of Water-Aluminum oxide nanofluid with different nanoparticle volume fractions in a three-dimensional rectangular microchannel. *Adv Mech Eng*, 7: 1-11.

AL-Ashhab, S. (2019) Asymptotic Behaviour and Existence of Similarity Solutions for a Boundary Layer Flow Problem. *Kuwait Journal of Science*, 46(2), 13-20.

AL-Hajri, S., Mahmood, S.M., Akbari, S., Abdulelah, H., Yekeen, N. & Saraih, N. (2020) Experimental investigation and development of correlation for static and dynamic polymer adsorption in porous media. *J Pet Sci Eng*, 189: 1058-1064.

AL-Jawary, M. (2020) Three iterative methods for solving Jeffery-Hamel flow problem. *Kuwait Journal of Science*, 47(1): 1-13.

Aminossadati, M. S., Raisi, A., & Ghasemi, B. (2011) Effects of magnetic field on nanofluid forced convection in a partially heated microchannel. *Int. J. Non Linear Mech*, 46: 1373-1382.

Behnampour, A., Akbari, O. A., Safaei, M. R., Ghavami, M., Marzban, A., Shabani, G. A. S., Zarringhalam, M. & Mashayekhi, R. (2017) Analysis of heat transfer and nanofluid fluid flow in microchannels with trapezoidal, rectangular and triangular shaped ribs. *Phys E*, 91: 15-31.

Boudiaf, A., Danane, F., Benkahla, Y.K., Berabou, W., Benzema, M. & Ouyahia, S. E. (2020) Heat transfer analysis of nanofluid flow through backward facing step. *MATECWeb Conf*, 307: 01-10.

Corcione, M. (2010) Heat transfer features of buoyancy-driven nanofluids inside rectangular enclosures differentially heated at the sidewalls. *Int. J. Thermal Sci*, 49(9): 1536-1546.

Dyachenko, A. Y., Zhdanov, V. L., Smulskii, Y. I. & Terekhov, V. I. (2019) Experimental investigation of heat transfers in the separation zone behind a backward-facing step in the presence of tabs. *Thermophys Aero-mech*, 26: 509-518.

Galuppo, W. C. & De, L. M. J. S. (2017) Turbulent heat transfers past a sudden expansion with a porous insert using a nonlinear model. *Numer Heat Transf Part Appl*, 71: 290-310.

Hilo, A. K., Abu, T. A. R., Acosta, I. A., Hameed, S. M. T. & Abdul, H. M. F. (2020) Effect of corrugated wall combined with backward-facing step channel on fluid flow and heat transfer. *Energy*, 190: 1162-1194.

Joibary, S. M. M. & Siavashi, M. (2019) Effect of Reynolds asymmetry and use of porous media in the counterflow double-pipe heat exchanger for passive heat transfer enhancement. *J Therm Anal Calorim*, 140: 1079-1093.

Kiran, S., Mani, S. & Sivanandam, S. (2021) Numerical study on conjugate convective thermal transport in an annular porous geometry. *Kuwait Journal of Science*, <https://doi.org/10.48129/kjs.10789>

Maghsoudi, P. & Siavashi, M. (2019) Application of nanofluid and optimization of pore size arrangement of heterogeneous porous media to enhance mixed convection inside a two-sided lid-driven cavity. *J Therm Anal Calorim*, 135: 947-961.

Martin, A. R., Saltiel, C. & Shyy, W. (1998) Heat transfer enhancement with porous inserts in recirculating flows. *J Heat Transf*, 120: 458-467.

Menouer, A., Chemloul, S. N. & Chaib, A. K. (2019) Steady Flow of Purely Viscous Shear-Thinning Fluids in a 1:3 Planar Gradual Expansion. *Journal of Applied Fluid Mechanics*, 12(3): 789-801.

Mostafavi, M. & Meghdadi, A. H. (2017) New Formulation for Prediction of Permeability of Nano Porous Structures using Lattice Boltzmann Method. *Journal of Applied Fluid Mechanics*, 10(2): 639- 649.

Naphon, P. (2007) Heat transfer characteristics and pressure drop in channel with V corrugated upper and lower plates. *Energy Convers Manag*, 48: 1516-1524.

Norouzi, A. M., Siavashi, M. & Khaliji, O. M. (2020) Efficiency enhancement of the parabolic trough solar collector using the rotating absorber tube and nanoparticles. *Renew Energy*, 145: 569-584.

Patel, E. H., Sundararajan, T., Pradeep, T., Dasgupta, A., Dasgupta, N. & Das, K. S. (2005) A micro-convection model for thermal conductivity of nanofluids. *Pramana- J. Phys*, 65 (5): 863-869.

Oliveira, J. P. (2003) Asymmetric flows of viscoelastic fluids in symmetric planar expansion geometries. *J. Non-Newtonian Fluid Mech*, 114: 33-63.

Rashidi, S., Karimi, N., Mahian, O. & Abolfazli, E. J. (2019) A concise review on the role of nanoparticles upon the productivity of solar desalination systems. *J Therm Anal Calorim*, 135: 1145-1159.

Saha, S., Biswas, P. & Nath, S. (2020) Bifurcation phenomena for incompressible laminar flow in expansion channel to study Coanda effect. *Journal of Interdisciplinary Mathematics*, 23 (2): 493-502.

Saha, S., Biswas, P., Rout, S. & Das, N. A. (2021a) Convective heat transfer of laminar nano-fluids flow through a rectangular micro-channel with different types of baffle-corrugation. *International Journal for Computational Methods in Engineering Science & Mechanics*, 22 (2): doi.org/10.1080/15502287.2021.1894509.

Saha, S., Rout, S. & Das, N. A. (2021b). Thermal enhancement and entropy generation of laminar water-Al₂O₃ nano-fluid flow through a sudden expansion channel with bell-shaped surface. *International Journal of Fluid Mechanic Research*, 48 (3): 65-78.

Soueid, A. A., Revil, A., Bolve, A., Steck, B., Vergnault, C. & Courivaud, J. R. (2020) Determination of the permeability of seepage flow paths in dams from self-potential measurements. *Eng Geol*, 268: 1055-1064.

Ternik, P., Marn, J. & Zunic, Z. (2006) Non-Newtonian Fluid Flow through a Planar Symmetric Expansion: Shear-thickening Fluids. *Journal of Non-Newtonian Fluid Mechanics*, 13: 136-148.

Terekhov, V. V. & Terekhov, V. I. (2017) Effect of surface permeability on the structure of a separated turbulent flow and heat transfer behind a backward-facing step. *J Appl Mech Tech Phys*. 58: 254-263.

Wei, B., Zhang, X., Liu, J., Xu, X., Pu, W. & Bai, M. (2020) Adsorptive behaviors of supercritical CO₂ in tight porous media and triggered chemical reactions with rock minerals during CO₂-EOR and sequestration. *Chem Eng J*, 381: 1225-1237.

Submitted: 29/07/2021

Revised: 02/12/2021

Accepted: 05/01/2022

DOI: 10.48129/kjs.15461